Lipids associated with plant-bacteria interaction identified using a metabolomics approach in an *Arabidopsis thaliana* model

Jian-Bo Song [1,2], **Rui-Ke Huang** [1,2], **Miao-Jie Guo** [1,2], **Qian Zhou** [3], **Rui Guo** [1,2], **Shu-Yuan Zhang** [1,2], **Jing-Wen Yao** [1,2], **Ya-Ni Bai** [1,2], **Xuan Huang** [Corresp. 1,2]

[1] College of Life Science, Northwest University, Shaanxi, Xi'an, China

[2] Key Laboratory of Resource Biology and Biotechnology in Western China (Ministry of Education), Provincial Key Laboratory of Biotechnology of Shaanxi, Shaanxi, Xi'an, China

[3] Shanghai Omicsspace Biotechnology Co.Ltd., Shanghai, Shanghai, China

Corresponding Author: Xuan Huang
Email address: xuanhuang@nwu.edu.cn

Background. Systemic acquired resistance (SAR) protects plants against a wide variety of pathogens. In recent decades, numerous studies have focused on the induction of SAR, but its molecular mechanisms remain largely unknown. **Methods.** We used a metabolomics approach based on ultra-high-performance liquid chromatographic (UPLC) and mass spectrometric (MS) techniques to identify SAR-related lipid metabolites in an *Arabidopsis thaliana* model . Multiple statistical analyses were used to identify the differentially regulated metabolites . **Results.** Numerous lipids were implicated as potential factors in both plant basal resistance and SAR; these include species of phosphatidic acid (PA), monogalactosyldiacylglycerol (MGDG), phosphatidylcholine (PC), phosphatidylethanolamine (PE), and triacylglycerol (TG). **Conclusions.** Our findings indicate that lipids accumulated in both local and systemic leaves, while other lipids only accumulated in local leaves or in systemic leaves. PA (16:0_18:2), PE (34:5) and PE (16:0_18:2) had higher levels in both local leaves inoculated with *Psm ES4326* or *Psm avrRpm1* and systemic leaves of the plants locally infected with *Psm avrRpm1* or *Psm ES4326*. PC (32:5) had high levels in leaves inoculated with *Psm ES4326*. Other differentially regulated metabolites, including PA (18:2_18:2), PA (16:0_18:3), PA (18:3_18:2), PE (16:0_18:3), PE (16:1_16:1), PE (34:4) and TGs showed higher levels in systemic leaves of the plants locally infected with *Psm avrRpm1* or *Psm ES4326*. These findings will help direct future studies on the molecular mechanisms of SAR.

1 **Lipids associated with plant-bacteria interaction identified using a metabolomics**
2 **approach in an *Arabidopsis thaliana* model**
3 Jian-Bo Song[1,2], Rui-Ke Huang[1,2], Miao-Jie Guo[1,2], Qian Zhou[3], Rui Guo[1,2], Shu-Yuan Zhang[1,2],
4 Jing-Wen Yao[1,2], Ya-Ni Bai[1,2], Xuan Huang[1,2*]
5 [1]Provincial Key Laboratory of Biotechnology of Shaanxi, Key Laboratory of Resource Biology
6 and Biotechnology in Western China (Ministry of Education), Xi'an, China.
7 [2]College of Life Sciences, Northwest University, Xi'an, China.
8 [3]Shanghai Omicsspace Biotechnology Co.Ltd., Shanghai, People's Republic of China
9 [*] Corresponding author: Xuan Huang (email: xuanhuang@nwu.edu.cn; phone: 15353647993).

11 **Abstract**
12 **Background.** Systemic acquired resistance (SAR) protects plants against a wide variety of
13 pathogens. In recent decades, numerous studies have focused on the induction of SAR, but its
14 molecular mechanisms remain largely unknown.
15 **Methods.** We used a metabolomics approach based on ultra-high-performance liquid
16 chromatographic (UPLC) and mass spectrometric (MS) techniques to identify SAR-related lipid
17 metabolites in an *Arabidopsis thaliana* model. Multiple statistical analyses were used to identify
18 the differentially regulated metabolites.
19 **Results.** Numerous lipids were implicated as potential factors in both plant basal resistance and
20 SAR; these include species of phosphatidic acid (PA), monogalactosyldiacylglycerol (MGDG),
21 phosphatidylcholine (PC), phosphatidylethanolamine (PE), and triacylglycerol (TG).
22 **Conclusions.** Our findings indicate that lipids accumulated in both local and systemic leaves,
23 while other lipids only accumulated in local leaves or in systemic leaves. PA (16:0_18:2), PE
24 (34:5) and PE (16:0_18:2) had higher levels in both local leaves inoculated with *Psm ES4326* or
25 *Psm avrRpm1* and systemic leaves of the plants locally infected with *Psm avrRpm1* or *Psm*
26 *ES4326*. PC (32:5) had high levels in leaves inoculated with *Psm ES4326*. Other differentially
27 regulated metabolites, including PA (18:2_18:2), PA (16:0_18:3), PA (18:3_18:2), PE
28 (16:0_18:3), PE (16:1_16:1), PE (34:4) and TGs showed higher levels in systemic leaves of the
29 plants locally infected with *Psm avrRpm1* or *Psm ES4326*. These findings will help direct future
30 studies on the molecular mechanisms of SAR.
31
32 **Keywords:** systemic acquired resistance, lipids, monogalactosyldiacylglycerol, phosphatidic
33 acid, phosphatidylethanolamine, triacylglycerol.

Introduction

35

36 A wide variety of pathogens have evolved to infect plants. Plant pathogens are divided into three
37 categories on the basis of their infection mode: biotrophic, necrotrophic, and hemibiotrophic.
38 Biotrophic pathogens infect specific types of plants to obtain nutrients required for growth
39 (Glazebrook 2005). Necrotrophic pathogens kill plants through the infection process and then
40 obtain nutrients from the dead plant cells (Mengiste 2012; Weiberg et al. 2014). Hemibiotrophic
41 pathogens grow and multiply by infecting plant cells and then subsequently kill the plant. There
42 are two types of plant immunity triggered by pathogens: pathogen-associated molecular pattern
43 (PAMP)-triggered immunity (PTI) and effector-triggered immunity (ETI). PTI, the most basic
44 type, is induced by pathogens entering through wounds or stomata (Chisholm et al. 2006).
45 Conserved features of the pathogens are recognized by the plant pattern-recognition receptors
46 (PRRs), triggering PTI through the accumulation of reactive oxygen species (ROS), increased
47 mitogen-activated protein kinase (MAPK) signaling, and alteration of calcium ion (Ca^{2+})
48 concentration. These all lead to the initiation of antimicrobial proteins, accumulation of
49 phytoalexins, as well as callose deposits (Adigun et al. 2021; Nürnberger et al. 2004).
50 Hemibiotrophic pathogens such as *Pseudomonas syringae* have evolved type III secretion
51 systems, whereby the pathogens inject effector molecules into the plant cytoplasm to suppress
52 PTI (Chang et al. 2005; Thomma et al. 2011). In response to such suppression, resistance
53 proteins (R proteins) of the nucleotide-binding site/leucine-rich repeat type (NBS-LRR) trigger
54 ETI by acting as intracellular receptor proteins (Dangl & Jones 2001). PTI and ETI often occur
55 synergistically and both can trigger strong immune responses and systemic acquired resistance
56 (SAR) (Ngou et al. 2021).
57   SAR is a defense mechanism that provides protection against a wide range of pathogens in
58 distal uninoculated leaves (Kachroo & Kachroo 2020; Kachroo & Robin 2013). During the
59 establishment period of SAR, some mobile signals from pathogen-infected tissues are transferred
60 to distal tissues through the phloem, including glycerol-3-phosphate (G3P) (Chanda et al. 2011),
61 azelaic acid (AzA) (Jung et al. 2009), pipecolic acid (Návarová et al. 2012), and *N*-
62 hydroxypipecolic acid (NHP) (Hartmann & Zeier 2018). Certain gaseous signaling molecules
63 volatilized by plants (*e.g.*, terpenes and methylsalicylic acid) can act as mobile signals to induce
64 resistance in adjacent plants (Wang et al. 2014). Besides these small molecules, several proteins
65 related to signal transportation are involved in the activation of defense responses by distal
66 tissues; for example, long distance transportation of the lipid transfer protein, DEFECTIVE IN
67 INDUCED RESISTANCE1 (DIR1), plays a key role in systemic immunity (Carella et al. 2015;
68 Champigny et al. 2013; Chanda et al. 2011; Wang et al. 2014).
69   Metabolomics approaches based on ultra-high-performance liquid chromatography (UPLC-
70 MS/MS) are increasingly being used for the elucidation of metabolites involved in the
71 development, biotic and abiotic stress responses of plants. These methods allow for precise
72 qualitative and quantitative analysis of primary and secondary compounds. Chernova *et al*.
73 utilized UPLC-MS/MS to demonstrate that triacylglycerols play essential roles in cold tolerance
74 mechanisms by comparing winter-type vs. spring-type plants (Chernova et al. 2018). Ward *et al*.

75   showed that the levels of phenolic, indolic, and amino acids in *Arabidopsis thaliana* change
76   notably within 8 h of infection, based on UPLC-MS/MS data (De Vos et al. 2007). Gao *et al.*
77   identified metabolites associated with systemic acquired resistance in *Arabidopsis* based on
78   UPLC-MS/MS data (Gao et al. 2020). The plant defense responses to pathogenic
79   microorganisms are often related to substantial modifications of the lipidome, and several
80   previous studies have measured *Arabidopsis* leaf lipids after *P. syringae* infection (Kirik &
81   Mudgett 2009; Nandi et al. 2004; Nilsson et al. 2014; Vu et al. 2012). In contrast to the
82   significant advances in plant research using UPLC-MS/MS methods and a metabolomics
83   approach, few studies have used a lipidomics approach for investigating SAR. In the present
84   study, two phytopathogens were used to induce SAR, and SAR-related lipid metabolites were
85   identified using UPLC-MS/MS-based lipidomics approaches. Various PAs, PCs, PEs, and TGs
86   were identified in plant-bacterial interactions.

Materials & methods

Plant materials

89   *A. thaliana* plants of Col-0 were used for our experiments. Seed dormancy was broken by
90   treatment at 4 °C for 3 d, then the seeds were surface-sterilized in 10% NaClO for 10 min, rinsed
91   three times with sterile water, and sown on MS solid medium (pH 5.8). Seedlings (four leaves)
92   were transferred to pots containing a mixture of soil, perlite and vermiculite (8:3:1 v/v/v).
93   Growth conditions included a relative humidity of 65% and a 16 h light (photon flux density 70
94   μmol m^{-2} s^{-1})/8 h dark cycle at 22 °C. Four-week-old plants that exhibited a uniform appearance
95   were used for SAR experiments.

Analyses of local and systemic resistance

97   *Arabidopsis* leaves were inoculated (by a syringe without needle) with avirulent *P. syringae pv.*
98   *maculicola ES4326* harboring avrRpm1 (*Psm avrRpm1*) or virulent *P. syringae pv. maculicola*
99   *ES4326* (*Psm ES4326*). The bacteria were grown at 28 °C in King's B medium containing the
100   appropriate antibiotics (tetracycline 50 mg/L, streptomycin 50 mg/L) under permanent shaking
101   (200 r/min, 28 °C). Overnight log-phase cultures were centrifuged at 3000 rpm for 5 min, then
102   the cultures were diluted with 10 mM $MgSO_4$ to OD_{600}= 0.002. Three lower rosette leaves of 4-
103   wk-old plants were infected with *Psm avrRpm1*; leaves treated with 10 mM $MgSO_4$ were used as
104   control. On the 3rd day, three upper leaves of each plant were inoculated with *Psm ES4326*, the
105   bacterial numbers were quantified at 3d post infiltration and phenotypes were compared at 4d
106   post infiltration (Li et al. 2020a).

Extraction of lipid metabolites

108   SAR was induced by inoculating three lower leaves of each plant with *Psm avrRpm1* or *Psm*
109   *ES4326* suspension; leaves treated with 10 mM $MgSO_4$ were used as control (CK). After 48 h,
110   leaves injected with $MgSO_4$, *Psm avrRpm1* or *Psm ES4326* (respectively termed LL-CK, LL-A,
111   LL-V, leaves of developmental stages 4-6 as sample), and systemic leaves locally injected with
112   $MgSO_4$-, *Psm avrRpm1*- or *Psm ES4326* (termed SL-CK, SL-A, SL-V, leaves of developmental
113   stages 7-9 as sample) were collected to perform a LC-MS/MS and RT-qPCR analysis (Gao et al.
114   2020). Lipids were extracted according to the method as described previously (Lu et al. 2019; Lu

115   et al. 2018). Freeze-dried samples (each 50 mg) were ground in liquid nitrogen, then 1 mL

116   precooled extraction solution was added ($CHCl_3$/ CH_3OH/ 300 mM ammonium bicarbonate,

117   30:41.5:3.5, v/v/v). The samples were then shaken at 100 rpm for 12 h at 4 °C and centrifuged at

118   1000 x g for 2 min at 4 °C. The supernatant was collected, 0.5 mL 1 M KCl was added, then the

119   supernatant was centrifuged at 1000 x g for 2 min at 4 °C. The upper aqueous phase was then

120   removed and the sample was washed two times with 1 mL sterile water. After the upper aqueous

121   phase was removed, the lower organic phase was dried under a stream of nitrogen. These

122   samples were then dissolved in $(CH_3)_2CHOH$/ C_2H_3N/ H_2O (3:3:1, v/v/v), centrifuged at 1000 x

123   g for 2 min, and the supernatant was then used for a UPLC-MS/MS analysis. Quality control

124   (QC) samples were mixed with equal amounts of each extraction solution.

125   **LC-MS/MS analysis**

126   Samples were placed in an autosampler at 4 °C, and separated on a Dionex UltiMate-3000 with

127   C_{18} column: sample volume 3 μL, column temperature 45 ℃, flow rate 0.3 mL/min;

128   chromatographic mobile phase A: 0.1% formic acid/ acetonitrile (6:4, v/v); mobile phase B:

129   acetonitrile/ propanol (1:9, v/v). The gradient elution program: 0-0.5 min, B maintained at 37%;

130   1.5-13.5 min, B increased from 37% to 70%; 13.5-15 min, B increased from 70% to 75%; 15.5-

131   16.5 min, B increased linearly from 75% to 98%; 16.5-18 min, B maintained at 98%; 18-19 min,

132   B decreased from 98% to 37%; 19-20 min, B maintained at 37%. The substances separated by

133   UPLC were analyzed by Q-Exactive mass spectrometry. Samples were subjected to electrospray

134   ionization (ESI) to yield positive and negative ions. The ESI source conditions were as follows:

135   spray voltage (kV), 3.5 ESI+ and 3.2 ESI-; source temperature, 320 ℃; sheath gas flow rate

136   (Arb), 45; aux gas flow rate (Arb), 15; mass range (m/z), 150-2000; full MS resolution, 70000;

137   MS/MS resolution, 17500; TopN, 10; stepped NCE 15, 25, 35.

138   **Data analysis**

139   Raw data were processed to ensure the retention time, peak alignment, and extraction of peak

140   area were correct using the Lipidsearch 4.2.21 software program (Blasco et al. 2017; Breitkopf et

141   al. 2017). To determine metabolite structures, the precision mass matching (25ppm), MS and

142   MS/MS matching data were used to search the Lipid MAPS database. A multidimensional

143   statistical analysis was performed using the SIMCA-P14.1 software (Blasco et al. 2017). Results

144   were generated by an orthogonal partial least square discriminant analysis (OPLS-DA).

145   **Total RNA extraction and quantitative real-time PCR (RT-qPCR)**

146   Total RNAs of the samples were isolated using a TRIzol reagent (Invitrogen), and the

147   complementary DNA (cDNA) was synthesized using the PrimeScript First Strand cDNA

148   Synthesis Kit (Takara). The 10 μL total reaction volume for RT-qPCR included 1 μL cDNA, 5

149   μL FastStart Essential DNA Green Master (Roche), 2 μL gene-specific primer, and 2 μL sterile

150   water. The RT-qPCR program was as follows: denaturation at 95 °C for 10 min, 39 cycles of

151   denaturation at 95 °C for 10 s and annealing at corresponding temperature for 30 s. Fold changes

152   of various genes were calculated using the $2^{-\Delta\Delta Ct}$ method. AtACT8 was used as the reference

153   gene. Primer sequences are listed in Table 1.

Results

154

Systemic acquired resistance (SAR) experiments

155

The quality of the samples was assessed using the RT-qPCR measurement of accumulation

156

levels of both *PR1* and *PR5* transcripts in the systemic leaves locally injected with $MgSO_4$-, *Psm*

157

avrRpm1- or *Psm ES4326* (SL-CK, SL-A, SL-V). *PR1* and *PR5* levels were higher in the

158

systemic leaves of the plants locally infected with *Psm avrRpm1* or *Psm ES4326* compared to the

159

systemic leaves of the locally $MgSO_4$ treated plant (Figure 1A). Successful SAR induction was

160

confirmed by performing secondary infection with *Psm ES4326* on the systemic leaves of plants

161

locally injected with $MgSO_4$, *Psm avrRpm1* or *Psm ES4326*. Phenotypes were compared after 4

162

d. Compared with $MgSO_4$ treated plants, the systemic leaves of plants locally infected with *Psm*

163

avrRpm1 or *Psm ES4326* had a lower degree of chlorosis and a smaller necrosis area (Figure

164

1C). The number of bacteria in the systemic leaves of the plants locally infected with *Psm*

165

avrRpm1 or *Psm ES4326* were significantly lower than in $MgSO_4$-treated leaves (Figure 1B).

166

These findings confirm successful SAR induction by *Psm avrRpm1* or *Psm ES4326*. These

167

samples were subsequently used for the lipid metabolomics analysis.

168

OPLS-DA

169

OPLS-DA accurately reveals intrinsic differences by removing data unrelated to classification,

170

thus improving analytical precision. We obtained values of 0.996 for R^2Y (which reflects

171

interpretive ability of variable Y) and 0.994 for Q^2 (which reflects predictive ability of the

172

model), indicating that the OPLS-DA reliably explains the differences between the treatment and

173

control groups (Figure 2). The long distance between the treatment groups and control group

174

indicates that the systemic leaves of the plants locally infected with *Psm avrRpm1* or *Psm*

175

ES4326 produce some metabolites that are different from those in the systemic leaves of the

176

locally $MgSO_4$ treated plants (Figure 2). The short distance between the systemic leaves of the

177

plants locally infected with *Psm avrRpm1* or *Psm ES4326* indicates that *Psm avrRpm1* and *Psm*

178

ES4326 induce similar metabolites in systemic leaves (Figure 2).

179

Identification of differentially regulated metabolites (DRMs) associated with SAR

180

A total of 127 lipid metabolites were identified in infected leaves and distal uninoculated leaves

181

(supplementfile1). A heatmap analysis of the DRMs in the samples is shown in Figure 3. We

182

found from the heat map that PE (34:5), PE (34:4), PA (16:0_18:3), PE (16:1_16:1) accumulated

183

in the systemic leaves of the plants locally infected with *Psm avrRpm1*or *Psm ES4326*. PE

184

(16:0_18:2) and PE (34:5) accumulated in the local leaves infected with *Psm ES4326*. The

185

screening of DRMs is shown in Figure 4A (fold change< 0.83 or > 1.2; VIP> 1; p< 0.05). There

186

were 10 DRMs with increased abundance and 15 DRMs with decreased abundance in leaves

187

inoculated with *Psm ES4326* (LL-V vs. LL-CK), including MGDG (16:1_18:2), MGDG

188

(18:2_16:2), PA (18:2_18:2), PE (16:0_18:3), PC (36:2) and PE (34:5). There were 15 DRMs

189

with decreased abundance in leaves inoculated with *Psm avrRpm1* (LL-A vs. LL-CK), including

190

PC (36:3), MGDG (18:2_16:2), and PE (34:4). The DRMs with either increased or decreased

191

levels in infected leaves are presumably related to the plant-bacteria interaction. There were 19

192

DRMs in the systemic leaves of the locally *Psm avrRpm1*-infected plant (SL-A vs. SL-CK) and

193

194   30 DRMs in the systemic leaves of the locally *Psm ES4326*-infected plant (SL-V vs. SL-CK) that
195   showed significant changes, including PE (34:5), PA (16:0_18:3) and PE (16:1_16:1). Some
196   DRMs were identified in both the infected leaves and distal uninoculated leaves. A Venn
197   diagram analysis showed 8 DRMs commonly found in the leaves of plants inoculated with *Psm*
198   *avrRpm1* or *Psm ES4326* (LL-A vs. LL-CK and LL-V vs. LL-CK) and 9 DRMs commonly
199   found in the systemic leaves of the plants locally infected with *Psm avrRpm1* or *Psm ES4326*
200   (SL-A vs. LL-CK and SL-V vs. LL-CK) (Figure 4B). Because *Psm avrRpm1* and *Psm ES4326*
201   induce very similar SAR in Col-0, there were common DRMs induced by *Psm avrRpm1* and
202   *Psm ES4326* in systemic leaves, such as PE (34:5), PE (34:4), PA (16:0_18:3), and PE
203   (16:1_16:1) (Table 2).
204   **Quantitative analysis of expression of PA-, PC-, PE-, TG-, and MGDG-related genes**
205   To explore the expression level of genes related to lipid biosynthesis, we performed an RT-qPCR
206   analysis of expression levels in the bacterium-treated and distal uninoculated leaves of six genes
207   involved in the synthesis of PAs, MGDGs, PCs, PEs, and TGs (Figure 5). The genes were
208   selected based on their functions in the specific metabolic pathways that we identified. PA,
209   produced by the sequential acylation of G3P by acyltransferase (GPAT1), is the substrate for
210   CDP-DG synthesis. Monogalactosyldiacylglycerol synthase 1 (MGD1) is a key enzyme in
211   MGDG synthesis. *PECT1* (encodes a mitochondrial ethanolamine-phosphate
212   cytidylyltransferase) and *CCT1* (encodes a phosphorylcholine cytidylyltransferase) are essential
213   genes in PE and PC synthesis. Amino-alcohol phosphotransferase (AAPT1) simultaneously
214   catalyzes the synthesis of PC and PE. TG is synthesized by diacylglycerol acyltransferase
215   (DGAT1), using acyl-CoA as the acyl donor. We found that the expression level of *DGAT1* was
216   significantly higher in leaves inoculated with *Psm avrRpm1* compared to leaves treated with
217    $MgSO_4$, and that the *CCT1* transcript level was upregulated significantly in leaves inoculated
218   with *Psm ES4326* (Figure 5). *PECT1* expression levels did not differ significantly among the
219   local leaf groups, but were higher in the systemic leaves of the plants locally infected with *Psm*
220   *avrRpm1* or *Psm ES4326* than in the systemic leaves of the locally $MgSO_4$ treated plant. This
221   study found that the expression level of *GPAT1* was induced by both *Psm avrRpm1* and *Psm*
222   *ES4326* in both inoculated and systemic leaves.

Discussion

224   Systemic acquired resistance (SAR) provides defense protection against a wide range of pathogens
225   in whole plants following primary inoculation (Maldonado et al. 2002). During the past decade,
226   certain metabolites have been studied extensively at the transcriptional and metabolic levels, but
227   still little is known about lipid responses to *Psm* (Gruner et al. 2013; Schwachtje et al. 2018).
228   Attaran *et al* found that plants can induce the accumulation of the terpenoids (E,E)-4,8,12-
229   trimethyl-1,3,7,11-tridecatetraene (TMTT), β-ionone and α-farnesene after inoculation of virulent
230   or avirulent *P. syringae* strains; and they proved that pathogen-induced synthesis of TMTT is
231   controlled through jasmonic acid (JA)-dependent signaling, but is independent of a functional
232   salicylic acid (SA) pathway (Attaran et al. 2008). Griebel *et al* found that the accumulation of
233   phytosterol stigmasterol is a significant part of the plant metabolic process that occurs upon

234 bacterial leaf infection (Griebel & Zeier 2010). Stahl *et al* show that inoculation of *Arabidopsis*
235 leaves with the bacterial pathogen *Pseudomonas syringae* induces the expression of genes
236 involved in the early steps of tocopherol biosynthesis and triggers a strong accumulation of γ-
237 tocopherol, a moderate production of δ-tocopherol, and the generation of the benzoquinol
238 precursors of tocopherols (Stahl et al. 2019). The connection between arabidopsides and
239 *Pseudomonas syringae* has also been established in previous studies. Anderesson *et al* found that
240 the levels of arabidopsides were highest 4 hours after local leaves were infected by *P. syringae* but
241 found no significant differences in the changes of nonoxidized fatty acids during the experiments
242 (Andersson et al. 2006). These SAR-related lipid derivatives were not identified in this study likely
243 because of the varying sample collection times and the methods used for lipid extraction. The
244 previous methods for extracting SAR-related metabolites were aimed at extracting metabolites
245 rather than targeting lipids. We used a metabolomics approach based on high-resolution mass
246 spectrometry to identify new lipid metabolites related to the plant-pathogen interaction in both
247 local and systemic leaves. A multivariate statistical analysis revealed significant metabolomic
248 differences between *Arabidopsis* plants injected with *Psm* and those injected with $MgSO_4$. SAR-
249 related lipids were identified for the first time based on a LC-MS/MS-based lipidomics approach,
250 and numerous DRMs were identified in the plant-pathogen interaction; these included MGDG
251 (16:1_18:2) $_{FC(SL-V)=0.45}$, PA (18:2_18:2) $_{FC(SL-V)=4.21}$, PC (32:5) $_{FC(SL-V)=0.11}$, PE (16:1_16:1) $_{FC(SL-V)}$
252 $_{=11.89}$ and TG (16:0_18:3_18:3) $_{FC(SL-V)=2.5}$. We also performed a correlation analysis of DRMs
253 (supplementfile2). The results showed that some lipids have different correlations between local
254 leaves and systemic leaves. For example, there is a positive correlation between PE (34:5) $_{FC(LL-V)}$
255 $_{=1.95, FC(SL-V)=3.82}$ and PA (18:3_18:3) $_{FC(LL-V)=1.67, FC(SL-V)=7.36}$ in local and systemic leaves. PC (32:5)
256 $_{FC(SL-V)=0.11}$ and PE (34:5) $_{FC(SL-V)=3.82}$ are negatively correlated in systemic leaves, but positively
257 correlated in local leaves.

258 **Phosphatidic acid (PA)**
259 We observed increased levels of PA (18:2_18:2) $_{FC(SL-A)=6.19, FC(SL-V)=4.21}$ and PA (16:0_18:3)
260 $_{FC(SL-V)=11.89, FC(SL-A)=11.88}$ in the systemic leaves of plants locally infected with *Psm avrRpm1* or
261 *Psm ES4326*, reflecting the role of PAs in biotic stress (Table 2). PAs are important plant lipids
262 involved in regulating physiological processes (*e.g.*, protein phosphorylation, cell proliferation
263 and growth) and cell membrane composition. They also function as signaling molecules in
264 various metabolic pathways in response to biotic and abiotic stresses (Bargmann & Munnik
265 2006; Wang et al. 2006). Under various stress conditions in *A. thaliana*, phospholipase D (PLD)
266 hydrolyzes the phosphodiester bond at the phospholipid terminal to produce defense-signaling
267 molecules such as second-messenger PA (Adigun et al. 2021). PLD promotes phosphorylation of
268 downstream signaling factors by regulating G proteins, and helps convert extracellular signals
269 into intracellular signals (Zhao et al. 2007). PA levels are upregulated at the wound site and in
270 the surrounding undamaged areas in mechanically wounded castor bean leaves, and systemically
271 upregulated in soybean seedlings (Lee et al. 2001; Ryu & Wang 1996). PAs produced through
272 PLD catalysis play essential roles in plant-pathogen interactions, and PA levels are correlated
273 with PLD transcription levels (Wang et al. 2006). Torres Zabela *et al*. observed that PLD
274 transcription levels were upregulated in *A. thaliana* leaves infected by both virulent and avirulent

275 strains of *P. syringae pv. Tomato* (de Torres Zabela et al. 2002).

Monogalactosyldiacylglycerol (MGDG)

277 In this work, we observed decreased levels of MGDG (16:1_18:2) $_{FC(LL-V) =0.32, FC(LL-A) =0.73}$ and

278 MGDG (16:2_18:2) $_{FC(LL-V) =0.30, FC(LL-A) =0.65}$ in both leaves inoculated with *Psm ES4326* or *Psm*

279 *avrRpm1*, indicating the importance of these lipid metabolites in the plant-pathogen interaction

280 (Table 2). Galactolipids comprise ~80% of membrane lipids in plants (Kelly & Dörmann 2004).

281 MGDG, a unique galactolipid localized in the chloroplast thylakoid membrane, is synthesized by

282 MGD1, which transfers a galactose residue to diacylglycerol (Awai et al. 2001).

283 Digalactosyldiacylglycerol (DGDG) is subsequently synthesized by digalactosyldiacylglycerol

284 synthase1 (DGD1) catalysis (Dörmann et al. 1999; Froehlich et al. 2001). MGDG and DGDG

285 levels are altered in the chloroplast thylakoid membranes through exposure to abiotic stress (Du

286 et al. 2018; Li et al. 2020b). Dörmann *et al.* reported that these compounds play key roles in the

287 remodeling of membrane lipids under freezing stress (Dörmann et al. 1995). They are both

288 associated with SAR. Gao *et al.* found that they regulate SAR in differing ways and function

289 nonredundantly (Gao et al. 2014). DGDG is involved in nitric oxide (NO) synthesis during SAR,

290 whereas MGDG regulates the synthesis of AzA, which functions downstream of NO. The α-Gal-

291 β-Gal head of DGDG is essential for establishing SAR; DGDG with a β-Glc-β-Gal head is

292 unable to perform this function.

Phosphatidylcholine (PC)

294 In the present study, all detected PCs showed significant changes in LL-V relative to LL-CK,

295 including PC (36:2) $_{FC(LL-V) =0.39}$, PC (36:3) $_{FC(LL-V) =0.44}$ and PC (36:4) $_{FC(LL-V) =0.64}$ (Table 2). The

296 different levels of PCs in leaves inoculated with *Psm ES4326* were detected in leaves inoculated

297 with *Psm avrRpm1*; however, the levels of all PCs in leaves inoculated with *Psm avrRpm1* were

298 lower than in leaves treated with MgSO$_4$. A possible explanation is that the differing virulence

299 factor (*AvrRpm1*) secreted by T3SS in *Psm avrRpm1* and *Psm ES4326* result in differing PC

300 accumulation levels. PC is a major, fundamental membrane lipid in eukaryotes, but much less

301 has been reported on its role in prokaryotes (Aktas et al. 2010). Because it is not detectable in the

302 membranes of *Escherichia coli* and *Bacillus subtilis*, two well-studied model species, its function

303 in bacteria was not appreciated for many decades. However, studies of bacterial genome

304 sequences around 2003 revealed that PC is present in 10% of bacterial species (Sohlenkamp et

305 al. 2003). Subsequent studies of PC were focused on host-pathogen interactions (Comerci et al.

306 2006; Conde-Alvarez et al. 2006). Xiong *et al.* observed that *P. syringae* strains defective in PC

307 synthesis lost virulence for infecting plants, and suggested that the type III secretion system

308 (T3SS) is directly dependent on PC for full virulence (Xiong et al. 2014).

Phosphatidylethanolamine (PE)

310 We observed significantly increased levels of PEs, including PE (34:5) $_{FC(SL-V) =3.82, FC(SL-A) =3.74}$

311 and PE (16:1_16:1) $_{FC(SL-V) =11.89, FC(SL-A) =11.88}$ in the systemic leaves of locally SAR-induced

312 plants, suggesting involvement of these PEs in SAR establishment (Table 2). PE is an abundant

313 membrane phospholipid in both *Arabidopsis* and bacteria (Randle et al. 1969). Many bacteria are

314 able to split PE into phosphate and ethanolamine as a source of carbon and nitrogen (Blackwell

315 et al. 1976; Proulx & Fung 1969). The ethanolamine utilization operon (eut) encodes

316 ethanolamine ammonialyase, which breaks down ethanolamine into acetaldehyde and ammonia
317 (Bradbeer 1965a; Bradbeer 1965b). Utilization of ethanolamine in host-pathogen interactions is
318 evidenced by the upregulation of eut genes. Munch *et al*. observed upregulation of eutABC in
319 the hemolymph of *Galleria mellonella* (greater wax moth) infected by *Photorhabdus*
320 *luminescens*, suggesting a key role of ethanolamine during this host-pathogen interaction (Münch
321 et al. 2008). The upregulation of eut genes has also been reported in plant-pathogen interactions.
322 Yang *et al*. found that eutR expression was induced by plant pathogen *Erwinia chrysanthemi* in
323 spinach, and that a mutant eutR strain caused localized maceration of African violets, but did not
324 cause systemic infection (Yang et al. 2004). These findings indicate that ethanolamine plays
325 important roles in both pathogens and host plants.

326 **Triacylglycerol (TG)**

327 After the leaves were inoculated with *Psm ES4326* bacteria, we observed increased levels of TGs
328 in the systemic leaves of the locally *Psm ES4326*-infected plant, including TG (16:0_16:0_16:0)
329 $_{FC(SL-V)=1.70}$, TG (16:0_16:0_16:1) $_{FC(SL-V)=1.83}$, TG (16:0_18:1_18:1) $_{FC(SL-V)=2.16}$ and TG
330 (16:0_18:3_18:3) $_{FC(SL-V)=2.50}$. This result suggests that TGs may be important in this stage of
331 SAR (Table 2). Triacylglycerol accounts for ~15% of the dry weight of plant leaves (Sanjaya et
332 al. 2011; Winichayakul et al. 2013). It is a major stored energy source during seed germination
333 and also an important factor in adult plant development (Fan et al. 2013; Graham
334 2008).Triacylglycerol is involved in a variety of abiotic stresses, including desiccation tolerance
335 and freezing tolerance (Gasulla et al. 2013; Moellering et al. 2010). Under nitrogen deprivation
336 conditions, both plant vegetative tissues and seeds show an increased expression of both DGAT1
337 (diacylglycerol acyltransferase) and PDAT (phospholipid:diacylglycerol acyltransferase), the key
338 enzyme for triacylglycerol synthesis (Lee et al. 2018). Triacylglycerol accumulation has a clear,
339 protective effect against cell death in plants (Fan et al. 2017). Studies of biotic stress have shown
340 that increased levels of unusual fatty acids in triacylglycerol protect *Arabidopsis* against
341 predation by newly-hatched cabbage looper caterpillars (Tunaru et al. 2012).

342

343 **Conclusions**

344 Lipids are involved in a vast array of developmental processes and various stress responses in
345 plants. During bacterial infection of plants, plants resist pathogen attacks through innate immune
346 responses, which are initiated by cell surface-localized pattern-recognition receptors (PRRs) and
347 intracellular nucleotide-binding domain leucine-rich repeat containing receptors (NLRs) leading
348 to PTI and ETI. SAR is then initiated to enhance resistance to pathogenic bacteria in the systemic
349 leaves of plants locally infected with *Psm avrRpm1* or *Psm ES4326*. In the present study, we
350 used molecular biology and metabolomics approaches to investigate differentially regulated
351 metabolites (DRMs) during plant-pathogen interaction. Among the 127 identified metabolites, 17
352 and 22 DRMs showed significant changes in local leaves and systemic leaves, respectively
353 (Table 2). PC (32:5) were displayed in high abundance in leaves inoculated with *Psm ES4326*,
354 indicating these DRMs were induced in local leaves infected with *P. syringae*. Other DRMs,
355 including PA (18:2_18:2), PA (16:0_18:3), PA (18:3_18:2), PE (16:0_18:3), PE (16:1_16:1), PE

356 (34:4) and TGs were displayed in high abundance in systemic leaves of plants locally infected
357 with *Psm avrRpm1* or *Psm ES4326*. PA (16:0_18:2), PE (34:5) and PE (16:0_18:2) were
358 displayed in high levels in both local leaves inoculated with *Psm ES4326* or *Psm avrRpm1*and
359 systemic leaves of the plants locally infected with *Psm avrRpm1* or *Psm ES4326*.

360
361
362
363
364
365
366

References

368 **Adigun OA, Nadeem M, Pham TH, Jewell LE, Cheema M, and Thomas R. 2021.** Recent advances in bio-
369   chemical, molecular and physiological aspects of membrane lipid derivatives in plant pathology. *Plant Cell*
370   *Environ* **44:**1-16. 10.1111/pce.13904

371 **Aktas M, Wessel M, Hacker S, Klüsener S, Gleichenhagen J, and Narberhaus F. 2010.** Phosphatidylcholine
372   biosynthesis and its significance in bacteria interacting with eukaryotic cells. *Eur J Cell Biol* **89:**888-894.
373   10.1016/j.ejcb.2010.06.013

374 **Andersson MX, Hamberg M, Kourtchenko O, Brunnström A, McPhail KL, Gerwick WH, Göbel C, Feussner**
375   **I, and Ellerström M. 2006.** Oxylipin profiling of the hypersensitive response in Arabidopsis thaliana.
376   Formation of a novel oxo-phytodienoic acid-containing galactolipid, arabidopside E. *J Biol Chem*
377   **281:**31528-31537. 10.1074/jbc.M604820200

378 **Attaran E, Rostás M, and Zeier J. 2008.** Pseudomonas syringae elicits emission of the terpenoid (E,E)-4,8,12-
379   trimethyl-1,3,7,11-tridecatetraene in Arabidopsis leaves via jasmonate signaling and expression of the
380   terpene synthase TPS4. *Mol Plant Microbe Interact* **21:**1482-1497. 10.1094/mpmi-21-11-1482

381 **Awai K, Maréchal E, Block MA, Brun D, Masuda T, Shimada H, Takamiya K, Ohta H, and Joyard J. 2001.**
382   Two types of MGDG synthase genes, found widely in both 16:3 and 18:3 plants, differentially mediate
383   galactolipid syntheses in photosynthetic and nonphotosynthetic tissues in Arabidopsis thaliana. *Proc Natl*
384   *Acad Sci U S A* **98:**10960-10965. 10.1073/pnas.181331498

385 **Bargmann BO, and Munnik T. 2006.** The role of phospholipase D in plant stress responses. *Curr Opin Plant Biol*
386   **9:**515-522. 10.1016/j.pbi.2006.07.011

387 **Blackwell CM, Scarlett FA, and Turner JM. 1976.** Ethanolamine catabolism by bacteria, including Escherichia
388   coli. *Biochem Soc Trans* **4:**495-497. 10.1042/bst0040495

389 **Blasco H, Veyrat-Durebex C, Bocca C, Patin F, Vourc'h P, Kouassi Nzoughet J, Lenaers G, Andres CR,**
390   **Simard G, Corcia P, and Reynier P. 2017.** Lipidomics Reveals Cerebrospinal-Fluid Signatures of ALS.
391   Sci Rep **7:**17652. 10.1038/s41598-017-17389-9

392 **Bradbeer C. 1965a.** The clostridial fermentations of choline and ethanolamine. 1. Preparation and properties of
393   cell-free extracts. *J Biol Chem* **240:**4669-4674.

394 **Bradbeer C. 1965b.** The clostridial fermentations of choline and ethanolamine. II. Requirement for a cobamide
395   coenzyme by an ethanolamine deaminase. *J Biol Chem* **240:**4675-4681.

396 **Breitkopf SB, Ricoult SJH, Yuan M, Xu Y, Peake DA, Manning BD, and Asara JM. 2017.** A relative
397   quantitative positive/negative ion switching method for untargeted lipidomics via high resolution LC-
398   MS/MS from any biological source. Metabolomics **13.** 10.1007/s11306-016-1157-8
399 **Carella P, Isaacs M, and Cameron RK. 2015.** Plasmodesmata-located protein overexpression negatively impacts
400   the manifestation of systemic acquired resistance and the long-distance movement of Defective in Induced
401   Resistance1 in Arabidopsis. *Plant Biol (Stuttg)* **17:**395-401. 10.1111/plb.12234
402 **Champigny MJ, Isaacs M, Carella P, Faubert J, Fobert PR, and Cameron RK. 2013.** Long distance movement
403   of DIR1 and investigation of the role of DIR1-like during systemic acquired resistance in Arabidopsis.
404   *Front Plant Sci* **4:**230. 10.3389/fpls.2013.00230
405 **Chanda B, Xia Y, Mandal MK, Yu K, Sekine KT, Gao QM, Selote D, Hu Y, Stromberg A, Navarre D,**
406   **Kachroo A, and Kachroo P. 2011.** Glycerol-3-phosphate is a critical mobile inducer of systemic
407   immunity in plants. *Nat Genet* **43:**421-427. 10.1038/ng.798
408 **Chang JH, Urbach JM, Law TF, Arnold LW, Hu A, Gombar S, Grant SR, Ausubel FM, and Dangl JL. 2005.**
409   A high-throughput, near-saturating screen for type III effector genes from Pseudomonas syringae. *Proc*
410   *Natl Acad Sci U S A* **102:**2549-2554. 10.1073/pnas.0409660102
411 **Chernova A, Gubaev R, Mazin P, Goryunova S, Demurin Y, Gorlova L, Vanushkina A, Mair W, Anikanov**
412   **N, Martynova E, Goryunov D, Garkusha S, Mukhina Z, and Khaytovich P. 2018.** UPLC⁻MS
413   Triglyceride Profiling in Sunflower and Rapeseed Seeds. *Biomolecules* 9. 10.3390/biom9010009
414 **Chisholm ST, Coaker G, Day B, and Staskawicz BJ. 2006.** Host-microbe interactions: shaping the evolution of
415   the plant immune response. *Cell* **124:**803-814. 10.1016/j.cell.2006.02.008
416 **Comerci DJ, Altabe S, de Mendoza D, and Ugalde RA. 2006.** Brucella abortus synthesizes phosphatidylcholine
417   from choline provided by the host. *J Bacteriol* **188:**1929-1934. 10.1128/jb.188.5.1929-1934.2006
418 **Conde-Alvarez R, Grilló MJ, Salcedo SP, de Miguel MJ, Fugier E, Gorvel JP, Moriyón I, and Iriarte M.**
419   **2006.** Synthesis of phosphatidylcholine, a typical eukaryotic phospholipid, is necessary for full virulence of
420   the intracellular bacterial parasite Brucella abortus. *Cell Microbiol* **8:**1322-1335. 10.1111/j.1462-
421   5822.2006.00712.x
422 **Dangl JL, and Jones JD. 2001.** Plant pathogens and integrated defence responses to infection. *Nature* **411:**826-833.
423   10.1038/35081161
424 **de Torres Zabela M, Fernandez-Delmond I, Niittyla T, Sanchez P, and Grant M. 2002**. Differential expression
425   of genes encoding Arabidopsis phospholipases after challenge with virulent or avirulent Pseudomonas
426   isolates. *Mol Plant Microbe Interact* **15:**808-816. 10.1094/mpmi.2002.15.8.808
427 **De Vos RC, Moco S, Lommen A, Keurentjes JJ, Bino RJ, and Hall RD. 2007.** Untargeted large-scale plant
428   metabolomics using liquid chromatography coupled to mass spectrometry. *Nat Protoc* **2:**778-791.
429   10.1038/nprot.2007.95
430 **Dörmann P, Balbo I, and Benning C. 1999.** Arabidopsis galactolipid biosynthesis and lipid trafficking mediated
431   by DGD1. *Science* **284:**2181-2184. 10.1126/science.284.5423.2181
432 **Dörmann P, Hoffmann-Benning S, Balbo I, and Benning C. 1995.** Isolation and characterization of an
433   Arabidopsis mutant deficient in the thylakoid lipid digalactosyl diacylglycerol. *Plant Cell* **7:**1801-1810.
434   10.1105/tpc.7.11.1801
435 **Du ZY, Lucker BF, Zienkiewicz K, Miller TE, Zienkiewicz A, Sears BB, Kramer DM, and Benning C. 2018.**
436   Galactoglycerolipid Lipase PGD1 Is Involved in Thylakoid Membrane Remodeling in Response to

437   Adverse Environmental Conditions in Chlamydomonas. *Plant Cell* **30:**447-465. 10.1105/tpc.17.00446

438 **Fan J, Yan C, and Xu C. 2013.** Phospholipid:diacylglycerol acyltransferase-mediated triacylglycerol biosynthesis

439   is crucial for protection against fatty acid-induced cell death in growing tissues of Arabidopsis. *Plant J*

440   **76:**930-942. 10.1111/tpj.12343

441 **Fan J, Yu L, and Xu C. 2017.** A Central Role for Triacylglycerol in Membrane Lipid Breakdown, Fatty Acid β-

442   Oxidation, and Plant Survival under Extended Darkness. *Plant Physiol* **174:**1517-1530.

443   10.1104/pp.17.00653

444 **Froehlich JE, Benning C, and Dörmann P. 2001.** The digalactosyldiacylglycerol (DGDG) synthase DGD1 is

445   inserted into the outer envelope membrane of chloroplasts in a manner independent of the general import

446   pathway and does not depend on direct interaction with monogalactosyldiacylglycerol synthase for DGDG

447   biosynthesis. *J Biol Chem* **276:**31806-31812. 10.1074/jbc.M104652200

448 **Gao H, Zhou Q, Yang L, Zhang K, Ma Y, and Xu ZQ. 2020.** Metabolomics analysis identifies metabolites

449   associated with systemic acquired resistance in Arabidopsis. *PeerJ* **8:**e10047. 10.7717/peerj.10047

450 **Gao QM, Yu K, Xia Y, Shine MB, Wang C, Navarre D, Kachroo A, and Kachroo P. 2014.** Mono- and

451   digalactosyldiacylglycerol lipids function nonredundantly to regulate systemic acquired resistance in plants.

452   *Cell Rep* **9:**1681-1691. 10.1016/j.celrep.2014.10.069

453 **Gasulla F, Vom Dorp K, Dombrink I, Zähringer U, Gisch N, Dörmann P, and Bartels D. 2013.** The role of

454   lipid metabolism in the acquisition of desiccation tolerance in Craterostigma plantagineum: a comparative

455   approach. *Plant J* **75:**726-741. 10.1111/tpj.12241

456 **Glazebrook J. 2005.** Contrasting mechanisms of defense against biotrophic and necrotrophic pathogens. *Annu Rev*

457   *Phytopathol* **43:**205-227. 10.1146/annurev.phyto.43.040204.135923

458 **Graham IA. 2008.** Seed storage oil mobilization. *Annu Rev Plant Biol* **59:**115-142.

459   10.1146/annurev.arplant.59.032607.092938

460 **Griebel T, and Zeier J. 2010.** A role for beta-sitosterol to stigmasterol conversion in plant-pathogen interactions.

461   *Plant J* **63:**254-268. 10.1111/j.1365-313X.2010.04235.x

462 **Gruner K, Griebel T, Návarová H, Attaran E, and Zeier J. 2013.** Reprogramming of plants during systemic

463   acquired resistance. *Front Plant Sci* **4:**252. 10.3389/fpls.2013.00252

464 **Hartmann M, and Zeier J. 2018.** l-lysine metabolism to N-hydroxypipecolic acid: an integral immune-activating

465   pathway in plants. *Plant J* **96:**5-21. 10.1111/tpj.14037

466 **Jung HW, Tschaplinski TJ, Wang L, Glazebrook J, and Greenberg JT. 2009.** Priming in systemic plant

467   immunity. *Science* **324:**89-91. 10.1126/science.1170025

468 **Kachroo A, and Kachroo P. 2020.** Mobile signals in systemic acquired resistance. *Curr Opin Plant Biol* **58:**41-47.

469   10.1016/j.pbi.2020.10.004

470 **Kachroo A, and Robin GP. 2013.** Systemic signaling during plant defense. *Curr Opin Plant Biol* **16:**527-533.

471   10.1016/j.pbi.2013.06.019

472 **Kelly AA, and Dörmann P. 2004.** Green light for galactolipid trafficking. *Curr Opin Plant Biol* **7:**262-269.

473   10.1016/j.pbi.2004.03.009

474 **Kirik A, and Mudgett MB. 2009.** SOBER1 phospholipase activity suppresses phosphatidic acid accumulation and

475   plant immunity in response to bacterial effector AvrBsT. *Proc Natl Acad Sci U S A* **106:**20532-20537.

476   10.1073/pnas.0903859106

477 **Lee HG, Kim H, Suh MC, Kim HU, and Seo PJ. 2018.** The MYB96 Transcription Factor Regulates

478   Triacylglycerol Accumulation by Activating DGAT1 and PDAT1 Expression in Arabidopsis Seeds. *Plant*
479   *Cell Physiol* **59:**1432-1442. 10.1093/pcp/pcy073
480 **Lee S, Hirt H, and Lee Y. 2001.** Phosphatidic acid activates a wound-activated MAPK in Glycine max. *Plant J*
481   **26:**479-486. 10.1046/j.1365-313x.2001.01037.x
482 **Li D, Liu R, Singh D, Yuan X, Kachroo P, and Raina R. 2020a.** JMJ14 encoded H3K4 demethylase modulates
483   immune responses by regulating defence gene expression and pipecolic acid levels. *New Phytol* **225:**2108-
484   2121. 10.1111/nph.16270
485 **Li J, Liu LN, Meng Q, Fan H, and Sui N. 2020b.** The roles of chloroplast membrane lipids in abiotic stress
486   responses. *Plant Signal Behav* **15:**1807152. 10.1080/15592324.2020.1807152
487 **Lu S, Liu H, Jin C, Li Q, and Guo L. 2019.** An efficient and comprehensive plant glycerolipids analysis approach
488   based on high-performance liquid chromatography-quadrupole time-of-flight mass spectrometer. *Plant*
489   *Direct* **3:**e00183. 10.1002/pld3.183
490 **Lu S, Sturtevant D, Aziz M, Jin C, Li Q, Chapman KD, and Guo L. 2018.** Spatial analysis of lipid metabolites
491   and expressed genes reveals tissue-specific heterogeneity of lipid metabolism in high- and low-oil Brassica
492   napus L. seeds. *Plant J* **94:**915-932. 10.1111/tpj.13959
493 **Maldonado AM, Doerner P, Dixon RA, Lamb CJ, and Cameron RK. 2002.** A putative lipid transfer protein
494   involved in systemic resistance signalling in Arabidopsis. *Nature* **419:**399-403. 10.1038/nature00962
495 **Mengiste T. 2012. Plant immunity to necrotrophs.** *Annu Rev Phytopathol* **50:**267-294. 10.1146/annurev-phyto-
496   081211-172955
497 **Moellering ER, Muthan B, and Benning C. 2010.** Freezing tolerance in plants requires lipid remodeling at the
498   outer chloroplast membrane. *Science* **330:**226-228. 10.1126/science.1191803
499 **Münch A, Stingl L, Jung K, and Heermann R. 2008.** Photorhabdus luminescens genes induced upon insect
500   infection. *BMC genomics* **9:**229. 10.1186/1471-2164-9-229
501 **Nandi A, Welti R, and Shah J. 2004.** The Arabidopsis thaliana dihydroxyacetone phosphate reductase gene
502   SUPPRESSSOR OF FATTY ACID DESATURASE DEFICIENCY1 is required for glycerolipid
503   metabolism and for the activation of systemic acquired resistance. *Plant Cell* **16:**465-477.
504   10.1105/tpc.016907
505 **Návarová H, Bernsdorff F, Döring AC, and Zeier J. 2012.** Pipecolic acid, an endogenous mediator of defense
506   amplification and priming, is a critical regulator of inducible plant immunity. *Plant Cell* **24:**5123-5141.
507   10.1105/tpc.112.103564
508 **Ngou BPM, Ahn HK, Ding P, and Jones JDG. 2021.** Mutual potentiation of plant immunity by cell-surface and
509   intracellular receptors. *Nature* **592:**110-115. 10.1038/s41586-021-03315-7
510 **Nilsson AK, Johansson ON, Fahlberg P, Steinhart F, Gustavsson MB, Ellerström M, and Andersson MX.**
511   **2014.** Formation of oxidized phosphatidylinositol and 12-oxo-phytodienoic acid containing acylated
512   phosphatidylglycerol during the hypersensitive response in Arabidopsis. *Phytochemistry* **101:**65-75.
513   10.1016/j.phytochem.2014.01.020
514 **Nürnberger T, Brunner F, Kemmerling B, and Piater L. 2004.** Innate immunity in plants and animals: striking
515   similarities and obvious differences. *Immunol Rev* **198:**249-266. 10.1111/j.0105-2896.2004.0119.x
516 **Proulx P, and Fung CK. 1969.** Metabolism of phosphoglycerides in E. coli. IV. The positional specificity and
517   properties of phospholipase A. *Can J Biochem* **47:**1125-1128. 10.1139/o69-181
518 **Randle CL, Albro PW, and Dittmer JC. 1969.** The phosphoglyceride composition of Gram-negative bacteria and

519   the changes in composition during growth. *Biochim Biophys Acta* **187:**214-220. 10.1016/0005-
520   2760(69)90030-7

521   **Ryu SB, and Wang X. 1996.** Activation of phospholipase D and the possible mechanism of activation in wound-
522   induced lipid hydrolysis in castor bean leaves. *Biochim Biophys Acta* **1303:**243-250. 10.1016/0005-
523   2760(96)00096-3

524   **Sanjaya, Durrett TP, Weise SE, and Benning C. 2011.** Increasing the energy density of vegetative tissues by
525   diverting carbon from starch to oil biosynthesis in transgenic Arabidopsis. *Plant Biotechnol J* **9:**874-883.
526   10.1111/j.1467-7652.2011.00599.x

527   **Schwachtje J, Fischer A, Erban A, and Kopka J. 2018.** Primed primary metabolism in systemic leaves: a
528   functional systems analysis. *Sci Rep* **8:**216. 10.1038/s41598-017-18397-5

529   **Sohlenkamp C, López-Lara IM, and Geiger O. 2003.** Biosynthesis of phosphatidylcholine in bacteria. *Prog Lipid*
530   *Res* **42:**115-162. 10.1016/s0163-7827(02)00050-4

531   **Stahl E, Hartmann M, Scholten N, and Zeier J. 2019.** A Role for Tocopherol Biosynthesis in Arabidopsis Basal
532   Immunity to Bacterial Infection. *Plant Physiol* **181:**1008-1028. 10.1104/pp.19.00618

533   **Thomma BP, Nürnberger T, and Joosten MH. 2011.** Of PAMPs and effectors: the blurred PTI-ETI dichotomy.
534   *Plant Cell* **23:**4-15. 10.1105/tpc.110.082602

535   **Tunaru S, Althoff TF, Nüsing RM, Diener M, and Offermanns S. 2012.** Castor oil induces laxation and uterus
536   contraction via ricinoleic acid activating prostaglandin EP3 receptors. *Proc Natl Acad Sci U S A* **109:**9179-
537   9184. 10.1073/pnas.1201627109

538   **Vu HS, Tamura P, Galeva NA, Chaturvedi R, Roth MR, Williams TD, Wang X, Shah J, and Welti R. 2012.**
539   Direct infusion mass spectrometry of oxylipin-containing Arabidopsis membrane lipids reveals varied
540   patterns in different stress responses. *Plant Physiol* **158:**324-339. 10.1104/pp.111.190280

541   **Wang C, El-Shetehy M, Shine MB, Yu K, Navarre D, Wendehenne D, Kachroo A, and Kachroo P. 2014.** Free
542   radicals mediate systemic acquired resistance. *Cell Rep* **7:**348-355. 10.1016/j.celrep.2014.03.032

543   **Wang W, Cajigas IJ, Peltz SW, Wilkinson MF, and González CI. 2006.** Role for Upf2p phosphorylation in
544   Saccharomyces cerevisiae nonsense-mediated mRNA decay. *Mol Cell Biol* **26:**3390-3400.
545   10.1128/mcb.26.9.3390-3400.2006

546   **Weiberg A, Wang M, Bellinger M, and Jin H. 2014.** Small RNAs: a new paradigm in plant-microbe interactions.
547   *Annu Rev Phytopathol* **52:**495-516. 10.1146/annurev-phyto-102313-045933

548   **Winichayakul S, Scott RW, Roldan M, Hatier JH, Livingston S, Cookson R, Curran AC, and Roberts NJ.**
549   **2013.** In vivo packaging of triacylglycerols enhances Arabidopsis leaf biomass and energy density. *Plant*
550   *Physiol* **162:**626-639. 10.1104/pp.113.216820

551   **Xiong M, Long D, He H, Li Y, Li Y, and Wang X. 2014.** Phosphatidylcholine synthesis is essential for HrpZ
552   harpin secretion in plant pathogenic Pseudomonas syringae and non-pathogenic Pseudomonas sp. 593.
553   *Microbiol Res* **169:**196-204. 10.1016/j.micres.2013.06.009

554   **Yang S, Perna NT, Cooksey DA, Okinaka Y, Lindow SE, Ibekwe AM, Keen NT, and Yang CH. 2004.**
555   Genome-wide identification of plant-upregulated genes of Erwinia chrysanthemi 3937 using a GFP-based
556   IVET leaf array. *Mol Plant Microbe Interact* **17:**999-1008. 10.1094/mpmi.2004.17.9.999

557   **Zhao X, Chang AY, Toh EA, and Arvan P. 2007.** A role for Lte1p (a low temperature essential protein involved
558   in mitosis) in proprotein processing in the yeast secretory pathway. *J Biol Chem* **282:**1670-1678.
559   10.1074/jbc.M610500200

560
561 **Legends:**
562 **Figure 1:**
563 **Systemic acquired resistance (SAR) experiments**
564 (A) Expression analysis of *PR1* and *PR5* in systemic leaves of plants inoculated locally with *Psm*
565 *avrRpm1* or *Psm ES4326* in comparison with MgSO$_4$-treated plants. (B) Growth of virulent *Psm*
566 *ES4326* on systemic leaves of Col-0. Three lower rosette leaves of 4-wk-old plants of Col-0
567 genotype were injected with MgSO$_4$, *Psm avrRpm1*; 2 d later, upper systemic leaves were
568 injected with *Psm ES4326*. At 3 d, one leaf disc (diameter 5 mm) was taken from each infiltrated
569 systemic leaf. (C) Phenotypes resulting from secondary infection with *Psm ES4326* on distal
570 leaves of plants locally injected with *Psm avrRpm1, Psm ES4326*, or MgSO$_4$. V: *Psm ES4326*;
571 A: *Psm avrRpm1*; CK: MgSO$_4$; SL-A: systemic leaves of locally *Psm avrRpm1* inoculated
572 plants; SL-V: systemic leaves of locally *Psm ES4326* inoculated plants; SL-CK: systemic leaves
573 of locally MgSO$_4$ inoculated plants. Statistical significance was determined by t-test (P <0.05).
574 ** represents P<0.01.
575
576 **Figure 2:**
577 **OPLS-DA score plots of leaves injected with MgSO$_4$, *Psm avrRpm1*, or *Psm ES4326* and**
578 **distal leaves of plants locally injected with MgSO$_4$, *Psm avrRpm1*, or *Psm ES4326***
579 OPLS-DA score plots were performed to reveal intrinsic difference within the signals of
580 different groups. X-axis is the correlation coefficient between permuted and original response
581 variables, which represents the degree of randomization of response variable y. SL-A: systemic
582 leaves of locally *Psm avrRpm1* inoculated plants; SL-V: systemic leaves of locally *Psm ES4326*
583 inoculated plants; SL-CK: systemic leaves of locally MgSO$_4$ treated plants (SL-CK groups were
584 two biological replicates).
585
586 **Figure 3:**
587 **Clustering analysis of identified metabolites in leaves injected with MgSO$_4$, *Psm avrRpm1*,**
588 **or *Psm ES4326* and distal leaves of plants locally injected with MgSO$_4$, *Psm avrRpm1*, or**
589 ***PsmES4326*.**
590 Each square represents a metabolite; the color scale on the right represents the abundance of
591 lipids (red represents increased abundance, blue represents decreased abundance). The
592 phylogeny lines on the left represent the clustering analysis results of metabolites. The
593 abundance values were calculated by log$_{10}$ (SL-CK groups were two biological replicates).
594
595 **Figure 4:**
596 **Responses of *Arabidopsis* metabolites to *Psm avrRpm1* and *Psm ES4326* infection in local**
597 **leaves and distal leaves of plants inoculated locally with *Psm avrRpm1* or *Psm ES4326*.**
598 (A) Numbers of commonly increased or decreased levels of metabolites in leaves infected with
599 *Psm avrRpm1* or *Psm ES4326* (LL-V vs. LL-CK, LL-A vs. LL-CK) and distal leaves of plants
600 locally infected with *Psm avrRpm1* or *Psm ES4326* in comparison with MgSO$_4$-treated plants

601   (SL-V vs. SL-CK, SL-A vs. SL-CK). (B) Venn diagrams illustrating common metabolites in
602   leaves infected with *Psm ES4326* or *Psm avrRpm1* (LL-V vs. LL-CK and LL-A vs. LL-CK),
603   distal leaves of plants locally infected with *Psm ES4326* or *Psm avrRpm1* (SL-V vs. SL-CK and
604   SL-A vs. SL-CK), leaves infected with *Psm ES4326* or distal leaves of locally *Psm ES4326*-
605   infected plants (LL-V vs. LL-CK and SL-V vs. SL-CK), leaves infected with *Psm avrRpm1* and
606   distal leaves of locally *Psm avrRpm1*-infected plants (LL-A vs. LL-CK and SL-A vs. SL-CK).
607   V: *Psm ES4326*; A: *Psm avrRpm1*; CK: $MgSO_4$; SL-A: systemic leaves of locally *Psm avrRpm1*
608   inoculated plants; SL-V: systemic leaves of locally *Psm ES4326* inoculated plants; SL-CK:
609   systemic leaves of locally $MgSO_4$ inoculated plants.
610
611   **Figure 5:**
612   **Expression analyses of genes related to lipids biosynthesis by RT-qPCR following**
613   **treatments with *Psm avrRpm1* and $MgSO_4$.**
614   The leaves injected with $MgSO_4$, *Psm avrRpm1* or *Psm ES4326* (LL-CK, LL-A, LL-V) and
615   distal leaves of plants locally injected with $MgSO_4$, *Psm avrRpm1*, or *Psm ES4326* (SL-CK, SL-
616   A, and SL-V) were collected at 48h. Relative transcript abundance of *AAPT1, CCT1, DGAT1,*
617   *MGD1, GPAT1* and *PECT*1 were determined in local and distal leaves of Col-0 by RT-qPCR.
618   The RT-qPCR analysis has 3 biological replicates for each treatment. Statistical significance was
619   determined by one-way ANOVA (P <0.05). * represents P<0.05, ** represents P<0.01. V: *Psm*
620   *ES4326*; A: *Psm avrRpm1*; CK: $MgSO_4$; SL-A: systemic leaves of locally *Psm avrRpm1*
621   inoculated plants; SL-V: systemic leaves of locally *Psm ES4326* inoculated plants; SL-CK:
622   systemic leaves of locally $MgSO_4$ inoculated plants.
623
624   **Table 1:**
625   **Primers used in RT-qPCR analyses of *PR1* and *PR5* genes related to SAR, and of lipid-**
626   **related genes.**
627
628   **Table 2:**
629   **Differentially regulated metabolites (DRMs) in LL-A vs. LL-CK, LL-V vs. LL-CK, SL-A**
630   **vs. SL-CK, and SL vs. SL-CK.**

Figure 1

Systemic acquired resistance (SAR) experiments

(A) Expression analysis of *PR1* and *PR5* in systemic leaves of plants inoculated locally with *Psm avrRpm1* or *Psm ES4326* in comparison with $MgSO_4$-treated plants. (B) Growth of virulent *Psm ES4326* on systemic leaves of Col-0. Three lower rosette leaves of 4-wk-old plants of Col-0 genotype were injected with $MgSO_4$, *Psm avrRpm1*; 2 d later, upper systemic leaves were injected with *Psm ES4326*. At 3 d, one leaf disc (diameter 5 mm) was taken from each infiltrated systemic leaf. (C) Phenotypes resulting from secondary infection with *Psm ES4326* on distal leaves of plants locally injected with *Psm avrRpm1, Psm ES4326*, or $MgSO_4$. V: *Psm ES4326*; A: *Psm avrRpm1*; CK: $MgSO_4$; SL-A: systemic leaves of locally *Psm avrRpm1* inoculated plants; SL-V: systemic leaves of locally *Psm ES4326* inoculated plants; SL-CK: systemic leaves of locally $MgSO_4$ inoculated plants. Statistical significance was determined by t-test (P <0.05). ** represents P<0.01.
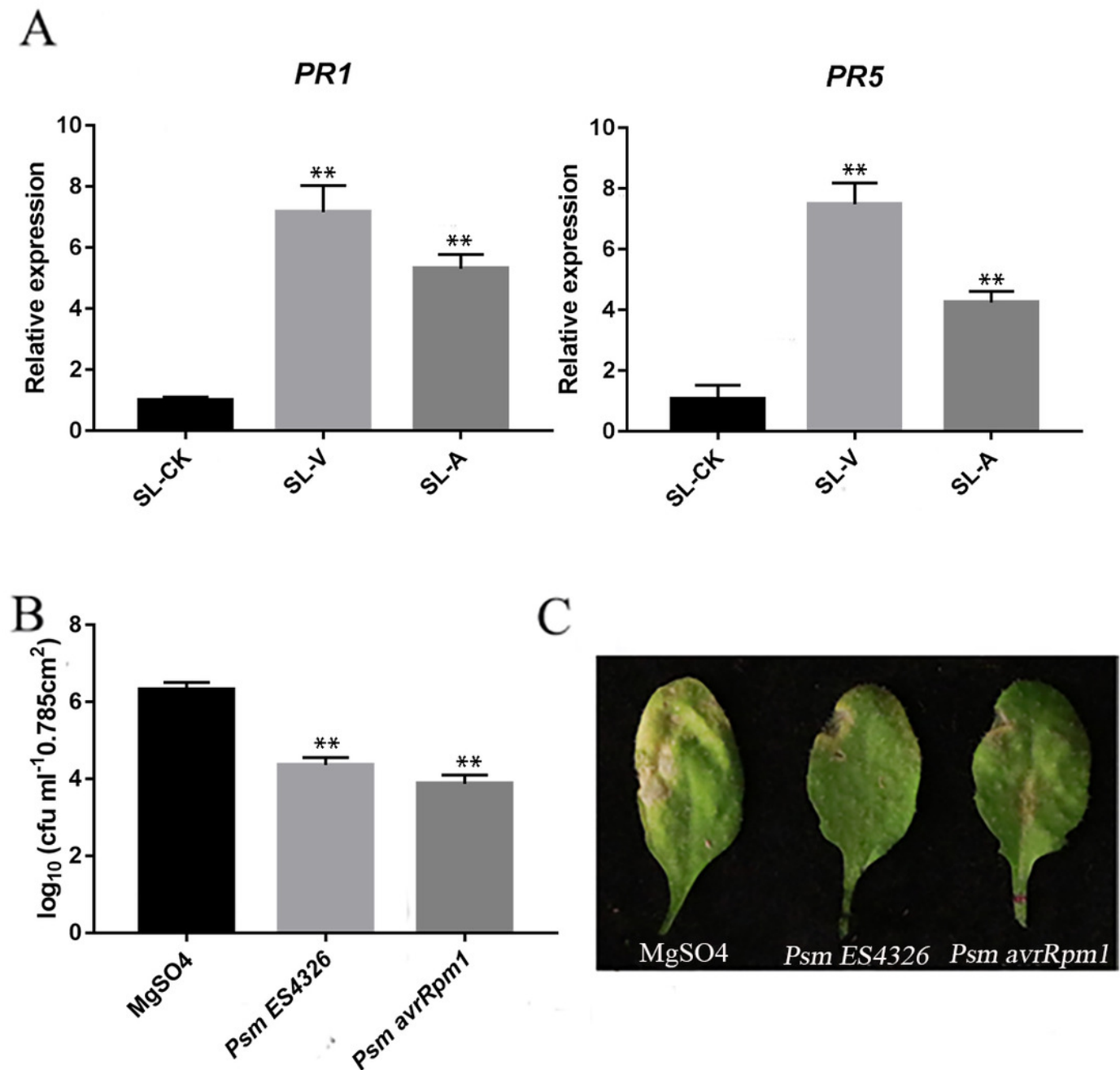
Figure 2

OPLS-DA score plots of leaves injected with MgSO$_4$, *Psm avrRpm1*, or *Psm ES4326* and distal leaves of plants locally injected with MgSO$_4$, *Psm avrRpm1*, or *Psm ES4326*

OPLS-DA score plots were performed to reveal intrinsic difference within the signals of different groups. X-axis is the correlation coefficient between permuted and original response variables, which represents the degree of randomization of response variable y. SL-A: systemic leaves of locally *Psm avrRpm1* inoculated plants; SL-V: systemic leaves of locally *Psm ES4326* inoculated plants; SL-CK: systemic leaves of locally MgSO$_4$ treated plants (SL-CK groups were two biological replicates).
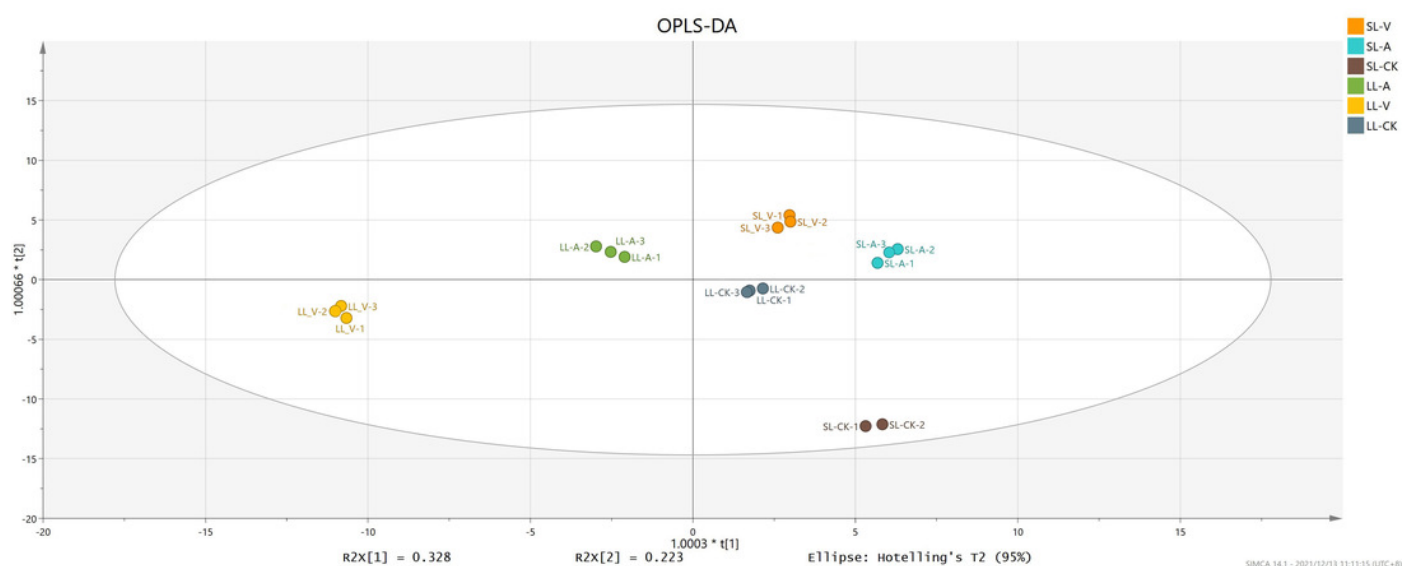
Figure 3

Clustering analysis of identified metabolites in leaves injected with MgSO₄, *Psm avrRpm1*, or *Psm ES4326* and distal leaves of plants locally injected with MgSO₄, *Psm avrRpm1*, or *PsmES4326*.

Each square represents a metabolite; the color scale on the right represents the abundance of lipids (red represents increased abundance, blue represents decreased abundance). The phylogeny lines on the left represent the clustering analysis results of metabolites. The abundance values were calculated by $\log_{10}$ (SL-CK groups were two biological replicates).

Heatmap of DRMs

PE(32:1)+Na
PC(32:5)+H
TG(16:0_18:1_18:1)+NH4
TG(16:0_16:0_18:2)+NH4
TG(16:0_16:0_16:1)+NH4
TG(16:0_16:0_18:1)+NH4
TG(16:0_16:0_16:0)+NH4
TG(16:0_16:1_16:1)+NH4
TG(18:1_18:1_18:1)+NH4
MGDG(18:2_16:2)+Na
PC(36:3)+H
MGDG(16:1_18:2)+Na
PA(18:2_18:2)+NH4
TG(16:0_18:3_18:3)+NH4
PE(34:5)+H
PC(36:2)+H
PE(18:2_18:2)+H
PE(16:0_18:2)+H
PC(36:4)+H
PE(16:0_18:3)+H
PA(16:0_18:3)+NH4
PE(16:1_16:1)+H
PE(34:4)+H
PA(18:3_18:2)+NH4

SL.V.1 SL.V.2 SL.V.3 SL.A.1 SL.A.2 SL.A.3 SL.CK.1 SL.CK.2 LL.V.1 LL.V.2 LL.V.3 LL.A.1 LL.A.2 LL.A.3 LL.CK.1 LL.CK.2 LL.CK.3

8.5
8
7.5
7
6.5

Figure 4

Responses of *Arabidopsis* metabolites to *Psm avrRpm1* and *Psm ES4326* infection in local leaves and distal leaves of plants inoculated locally with *Psm avrRpm1* or *Psm ES4326*.

(A) Numbers of commonly increased or decreased levels of metabolites in leaves infected with *Psm avrRpm1* or *Psm ES4326* (LL-V vs. LL-CK, LL-A vs. LL-CK) and distal leaves of plants locally infected with *Psm avrRpm1* or *Psm ES4326* in comparison with $MgSO_4$-treated plants (SL-V vs. SL-CK, SL-A vs. SL-CK). (B) Venn diagrams illustrating common metabolites in leaves infected with *Psm ES4326* or *Psm avrRpm1* (LL-V vs. LL-CK and LL-A vs. LL-CK), distal leaves of plants locally infected with *Psm ES4326* or *Psm avrRpm1* (SL-V vs. SL-CK and SL-A vs. SL-CK), leaves infected with *Psm ES4326* or distal leaves of locally *Psm ES4326*-infected plants (LL-V vs. LL-CK and SL-V vs. SL-CK), leaves infected with *Psm avrRpm1* and distal leaves of locally *Psm avrRpm1*-infected plants (LL-A vs. LL-CK and SL-A vs. SL-CK). V: *Psm ES4326*; A: *Psm avrRpm1*; CK: $MgSO_4$; SL-A: systemic leaves of locally *Psm avrRpm1* inoculated plants; SL-V: systemic leaves of locally *Psm ES4326* inoculated plants; SL-CK: systemic leaves of locally $MgSO_4$ inoculated plants.

A
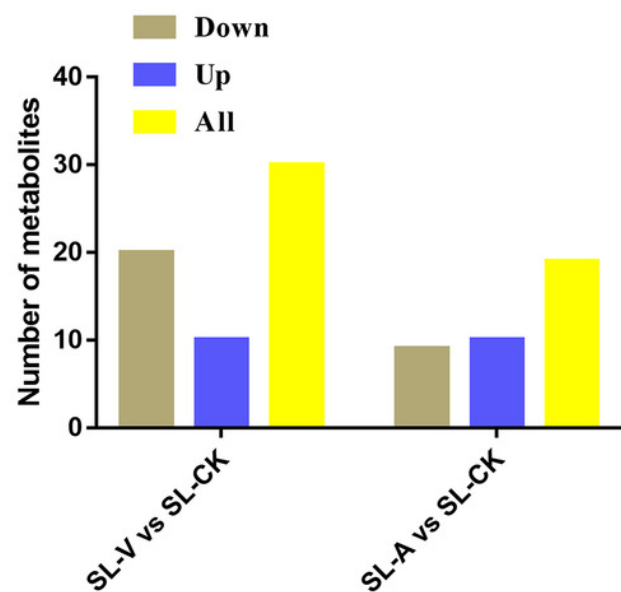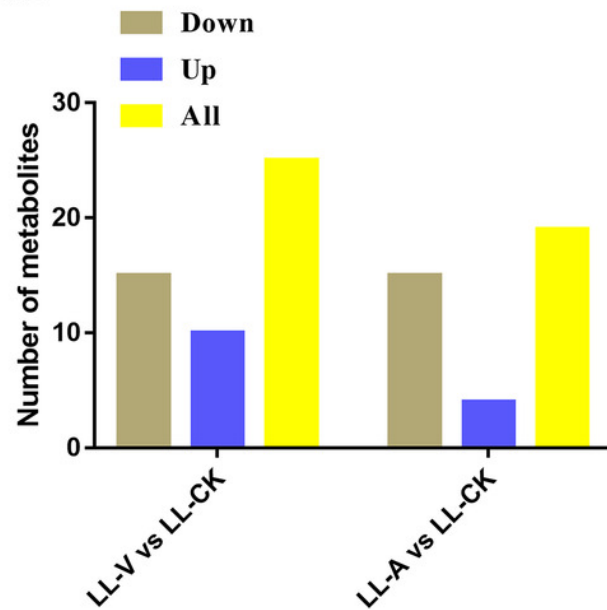
B
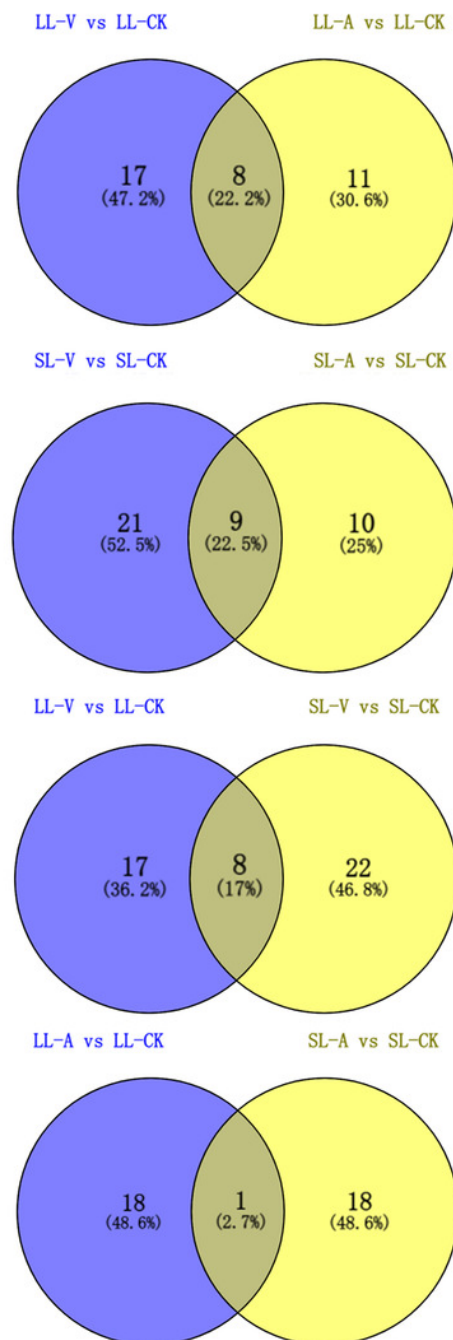
Figure 5

Expression analyses of genes related to lipids biosynthesis by RT-qPCR following treatments with *Psm avrRpm1* and MgSO$_4$.

The leaves injected with MgSO$_4$, *Psm avrRpm1* or *Psm ES4326* (LL-CK, LL-A, LL-V) and distal leaves of plants locally injected with MgSO$_4$, *Psm avrRpm1*, or *Psm ES4326* (SL-CK, SL-A, and SL-V) were collected at 48h. Relative transcript abundance of *AAPT1, CCT1, DGAT1, MGD1, GPAT1* and *PECT*1 were determined in local and distal leaves of Col-0 by RT-qPCR. The RT-qPCR analysis has 3 biological replicates for each treatment. Statistical significance was determined by one-way ANOVA (P <0.05). * represents P<0.05, ** represents P<0.01. V: *Psm ES4326*; A: *Psm avrRpm1*; CK: MgSO$_4$; SL-A: systemic leaves of locally *Psm avrRpm1* inoculated plants; SL-V: systemic leaves of locally *Psm ES4326* inoculated plants; SL-CK: systemic leaves of locally MgSO$_4$ inoculated plants.
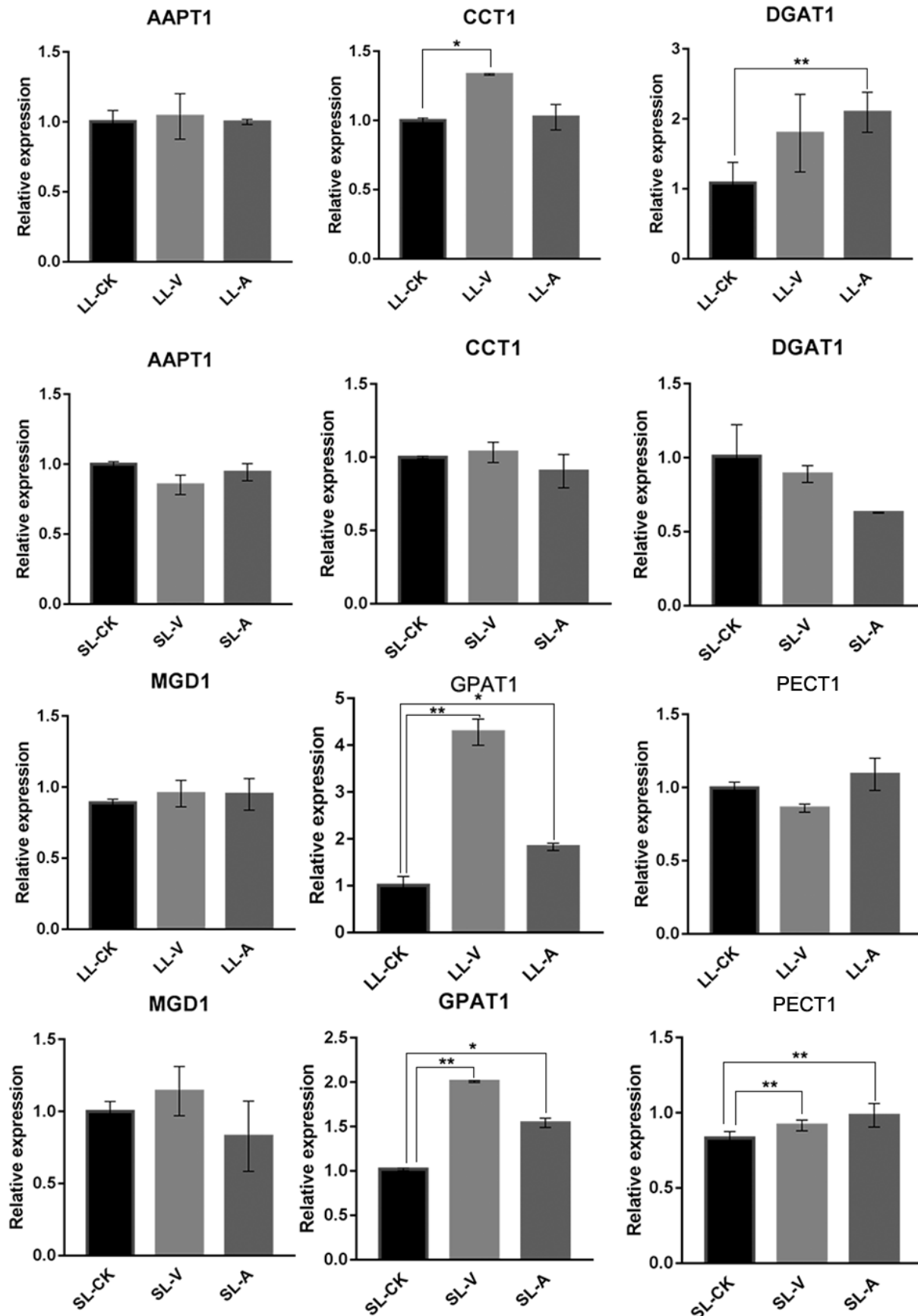
Primers used in RT-qPCR analyses of PR1 and PR5 genes related to SAR, and of lipid-related genes.

1   **Table 1**. Primers used in RT-qPCR analyses of PR1 and PR5 genes related to SAR, and of lipid-related genes.

Gene	Sequences of primers (5'→3')	Size of amplicon (bp)
MGD1 (AT4G31780)	F:GGAATGTATGGGTGCCTGTGACTG R: GCCTCTTGACCAGCGATGTAACC	117
GPAT1 (AT1G06520)	F:AGCCTGCACTTGGAATTGGAAGC R:TGCGTTGTTCTTGCTCATGGACTC	113
DGAT1 (AT2G19450)	F:TGGAAGAGGCGGCGGAGAAG R:TGAAGATTGCGTCGGAGCTAAGTG	116
AAPT1 (AT1G13560)	F:TGATGGGAAGCAAGCAAGAAGGA R:CACAAGCAAGCGCGTCACAAC	83
CCT1 (AT2G32260)	F:CGCACTGAAGACGGCCTTTCC R:TCGTAGATCCCATCGGCGTAGAC	110
PECT1 (AT2G38670)	F:CTTCGTCAAGCTCGTGCTCTCG R:AACTTCATCCACCCACTTCACAGC	144
PR1 (AT2G14610)	F: CTCTTGTAGGTGCTCTTGTTC R: CCTCTTAGTTGTTCTGCGTAG	160
PR5 (AT1G75040)	F:AAGAGTGCCTGTGAGAGGTT R:TTCGTCGTCATAAGCGTAGC	144
ACT8 (AT1G49240)	F: TGTGCCTATCTACGAGGGTTT R: TTTCCCGTTCTGCTGTTGT	137

Differentially regulated metabolites (DRMs) in LL-A vs. LL-CK, LL-V vs. LL-CK, SL-A vs. SL-CK, and SL vs. SL-CK.

2 **Table 2**. Differentially regulated metabolites (DRMs) in LL-A vs. LL-CK, LL-V vs. LL-CK, SL-A vs. SL-CK, and SL vs. SL-CK.

DLM	Formula	Fold change and p-value				
		LL-V vs. LL-CK	LL-A vs. LL-CK	SL-V vs. SL-CK	SL-A vs. SL-CK (min)	RT
MGDG (16:1_18:2)	C43 H76 O10	0.32(1.37E-02)	0.73(3.76E-02)		0.45(8.02E-03)	9.69
MGDG (16:2_18:2)	C43 H74 O10	0.30(2.90E-04)	0.65(2.26E-03)			9.43
PA (18:2_18:2)	C39 H73 O8 N1 P1	0.50(4.86E-03)	0.67(2.25E-02)	4.21(4.96E-02)	6.19(1.47E-03)	7.70
PA (16:0_18:3)	C37 H71 O8 N1 P1	0.79(1.05E-01)		11.89(6.35E-05)	11.88(5.67E-03)	8.97
PA (16:0_18:2)	C37 H73 O8 N1 P1	2.07(3.28E-01)	0.54(4.46E-03)		1.53(4.56E-01)	8.98
PA (18:3_18:2)	C39 H71 O8 N1 P1		0.69(3.18E-02)	1.93(1.92E-02)	2.30(3.33E-03)	7.83
PC (36:2)	C44 H85 O8 N1 P1	0.39(4.08E-03)	0.67(3.39E-02)			10.45
PC (36:3)	C44 H83 O8 N1 P1	0.44(2.09E-04)	0.64(1.77E-03)			9.89
PC (36:4)	C44 H81 O8 N1 P1	0.64(3.17E-03)	0.64(8.58E-03)		1.54(5.4E-02)	9.16
PC (32:5)	C40 H71 O8 N1 P1	6.70(3.27E-05)		0.11(1.97E-05)	0.16(2.84E-4)	7.21
PE (16:0_18:3)	C39 H73 O8 N1 P1	0.79(3.94E-02)	0.83(4.32E-2)	1.23(8.44E-04)	1.43(6.87E-02)	8.95
PE (34:5)	C39 H69 O8 N1 P1	1.95(2.30E-02)		3.82(1.14E-05)	3.74(2.31E-04)	8.34
PE (16:1_16:1)	C37 H71 O8 N1 P1	0.79(1.05E-01)		11.89(6.35E-05)	11.88(5.57E-03)	9.01
PE (16:0_18:2)	C39 H75 O8 N1 P1	1.51(4.24E-01)		1.19(1.35E-02)	1.36(1.01E-01)	10.02
PE (34:4)	C39 H71 O8 N1 P1		0.65(2.33E-03)	2.08(1.67E-03)	2.23(1.18E-02)	8.33
PE (18:2_18:2)	C41 H75 O8 N1 P1			1.24(2.41E-01)	1.73(3.48E-04)	8.50
TG (16:0_16:0_16:0)	C51 H102 O6 N1			1.70(2.77E-02)	1.32(1.92E-01)	15.14
TG (16:0_16:0_16:1)	C51 H100 O6 N1			1.83(2.03E-02)	1.47(2.14E-01)	14.74
TG (16:0_16:1_16:1)	C51 H98 O6 N1			1.73(6.22E-03)	1.47(2.83E-01)	14.53
TG (16:0_16:0_18:1)	C53 H104 O6 N1			1.75(1.45E-02)		15.06
TG (16:0_16:0_18:2)	C53 H102 O6 N1			1.78(2.36E-03)		14.82
TG (16:0_18:1_18:1)	C55 H106 O6 N1			2.16(6.11E-03)		15.05
TG (16:0_18:3_18:3)	C55 H98 O6 N1			2.50(7.76E-03)	1.90(6.16E-03)	13.89
TG (18:1_18:1_18:1)	C57 H108 O6 N1			1.71(2.17E-02)		15.1